Nuclear magnetic resonance and petrography correlations of anomalous porosity sandstones in the Recôncavo Basin

Marta Henriques Jácomo (IAG/USP)*, Carlson de Matos Maia Leite (RH/Universidade Petrobrás), Ricardo Ivan Ferreira da Trindade (IAG/USP), Everton Lucas de Oliveira (IFSc/USP), Tito Bonagamba (IFSc/USP)

Abstract

Microcrystalline quartz coating in sandstone is one of the processes resposible for porosity preservation in deep sliciclastic reservoirs. Despite numerous works on the coating structure, mineral texture and the mechanisms leading to porosity preservation, a detailed study of the porosity distribution in these rocks is still lacking. Here we apply nuclear magnetic ressonance (NMR) techniques and petrographic observations to address this problem. We analysed fluvial and eolian sandstones from the Agua Grande Formation (Recôncavo Basin), comprising two samples with anomalous porosity (reservoir) and a non-reservoir sandstone, where the porosity was obliterated by quartz overgrowth. We verified the existence of large (close to the relaxation times of bulk water) pores and micropores in reservoir samples, whereas the non-reservoir sample presents only micropororsity. By comparing our results with those of the well-characterized clean sanstone from Fontainebleau Formation, we interpret the bimodal porosity distributiuon as being related to the preserved macropores and to the intercrystalline microporosity in the quartz coating. NMR measurements and microscopic observations enable to map the size, distribution and interconnectivity between these two sites.

Introduction

Good porosity preservation can be a key element in the effectiveness of hydrocarbon reservoirs, particularly in deep reservoirs. The loss of porosity in sandstones at depth depends mostly on the mechanical compaction and quartz cementation during progressive burial. However, in some cases porosity obliteration is prevented due to fluid overpressure, low thermal maturity, early hydrocarbon emplacement and clay or quartz grain-coatings (Bloch et al., 2002). Anomalously high porosity caused by microcrystalline quartz coating in sandstones has been studied by many authors in different depositional settings (Worden et al., 2012; French & Worden, 2013; Hendry & Trewin, 1995; Hattori et al., 1996). These studies detailed the coating structure, mineral texture and suggest mechanisms leading to porosity preservation. A detailed study of the porosity distribution in these rocks is however lacking. A potential tool to be applied in this case is the nuclear magnetic resonance (NMR). NMR can be used to define porosity, pore size distribution, as well as physical properties at the pore-grain interface such as magnetic susceptibility and irreducible saturation of water (Mitchell et.al., 2013). In the present study we characterize the porosity space of samples from Água Grande Formation, which show anomalous porosity due to microcrystalline quartz coatings using both petrography (optical and electronic microscopy) and NMR.

Geological Setting

Recôncavo Basin, situated in Northeastern Brazil, is an aborted rift half graben related to the South Atlantic Ocean opening during the Early Cretaceous (Milani & Davison, 1988). It is one of the most productive onshore areas in Brazil, with 72 mature fields presently in operation (ANP, 2016). Recôncavo basin reservoirs can be assembled into four systems: 1) pre-rift aeolian fluvial sandstones of Candeias/Sergi and Água Grande Formations; 2) syn-rift deltaic sandstones of Candeias/Ilhas Group; 3) syn-rift turbidite sandstones of Candeias/Candeias Formation; 4) ryn-rift turbidite Candeias/ Maracangalha Formation (Magnavita et.al., 2012); the pre-rift system being the main reservoirs.The Candeias Formation is the hydrocarbon source for the petroleum system. It consists of rich organic carbon grayish lacustrine shales (average 4% and kerogen type 1) intercalated with mudstones, siltstones, limestones and dolomites (Magnavita etal.,2012).

Reservoir rocks of Água Grande Formation are related to eolian-fluvial sequences. The fluvial unit is composed of cycles of finning upward sequences with conglomeratic sandstones on the base and coarse to fine sandstone at the top. The top of the cycles consists of silty shales. The eolian unit is composed of well-sorted medium grained planar-bedded sandstones with grain falls structures (Cortez, 1996). This progradational context was has been interpreted as a drying upward cycle by Wiederkehr (2010).

Eolian sandstones have until 22% of intergranular primary porosity, while fluvial sandstones present intense chemical compaction and quartz cementation, significantly decreasing the original porosity (<18%). The high porosity preserved in the eolian sandstones is due to the presence of microquartz rims that inhibit quartz overgrowth (Leite et al., 2014). According to these authors, the precipitation of microquartz would have happened early in the diagenetic history, during percolation of alkaline solutions in semi-arid climate.

Methods and techniques

Transmitted-light optics

Blue epoxy-impregnated thin sections were examined with transmitted-light optical microscope for identifying the types of present minerals, the textural framework and the types of authigenesis of silica.

Porosity (ϕ) and permeability (k) mesurements

Porosity and permeability of samples were measured on each sample. Porosity was determined using optical,

Helium expansion 2500 PSI, density and RMN after saturation methods (Table 1). These values present a good correlation (except for petrographic ϕ). The permeability was determined using Hassler cell (Table 1).

Magnetic susceptibility measurements

Magnetic susceptibility differences caused by presence of paramagnetic minerals or impurities in rock samples can induce field inhomogeneity in the pore space, causing an increase in T2 relaxation rates (Washburn et al, 2008). Thus, these measurements are important to understand eventual contrasts on the T2 NMR response in porous media. We used the Susceptmeter KLY-4S-Kappabridge by AGICO operating at 976 Hz at IAG/USP (Brazil).

Nuclear Magnetic Resonance (NMR)

Examples of application of Nuclear Magnetic Resonance techniques to porous media are presented in Dastidar et al., (2010), Vincent et al. (2011), Mitchell et al. (2013) among others.

The NMR relaxation (T1 and T2) depends on several factors such uniformity of the magnetic field, presence of paramagnetic minerals, fluid-surface interaction and the rotational and translation diffusion. The exponential longitudinal relaxation (T1) is related to the return time of the magnetization to the z-axis and is influenced by the energy exchange between the excited spin and its molecular neighborhood (net) to thermal equilibrium. The transverse relaxation is related to the interaction between spins (spin-spin) and thus, to the exponential decay of magnetization in the transverse plane.

The pore space controls the relaxation process by three mechanisms: 1) intrinsic relaxation, which is controlled by viscosity, fluid composition, temperature and pressure and affect both T1 and T2; 2) surface relaxation, which is controlled by grain mineralogy and s/v ratio (size of pores), and occurs in T1 and T2; 3) molecular diffusion, which is controlled by the behavior of the fluids when submitted to a magnetic field gradient. The molecules diffuse into areas with a distinct magnetic field, making the precession rate different; it affects only T2.

The relation that governs surface mechanisms in the fast diffusion regime is:

$$1/T1=\rho1(s/v)\ \text{pore and}\ 1/T2=\rho2(s/v)\ \text{pore} \quad \text{(Eq.1)},$$

where T1 and T2 are the longitudinal and transverse relaxation times, ρ1 and ρ2 are the surface relaxivity for T1 and T2 respectively, s/v is the surface/volume ratio. Therefore, the larger the pore size the smaller the s/v ratio and the greater the relaxation time T2.

The total relaxation is a sum of decay signals of each pore size:

$$M_z(t)=\sum_{i=1}^{n} Mi \exp(-t/T_{2i}), \quad \text{(Eq.2)},$$

where Mi is the initial magnetization (Gauss) of the relaxation component, T2i is a constant decay time for the it pore and Mz (t) is the magnetization at time t.

The relaxation time rate due the molecular diffusion is given by:

$$\frac{1}{T_{2\,diffusion}} = \frac{D(\gamma GTE)^2}{12},$$

where $1/T_{2\ diffusion}$ is the relaxation time due the molecular diffusion rate, D is the molecular diffusion coefficient, γ is gyromagnetic constant, G is the magnetic field gradient (G / cm) and TE is the intercooled time used in the CPMG sequence measurements (Carr-Purcell-Meiboom-Gill).

NMR Measurements

T1, T2 and D were measured using known two-dimensional experiments T1-T2 and D-T2 (Song et al., 2002; Mitchel et al., 2013). T1-T2 is characterized by the sum of two sequences: Inversion-recovery for T1 and CPMG for T2, while D-T2 consists in Pulsed field gradient, stimulated echo (PFG-STE) sequence and then, CPMG. Figure 1 shows the pulse sequences utilized in our experiments.

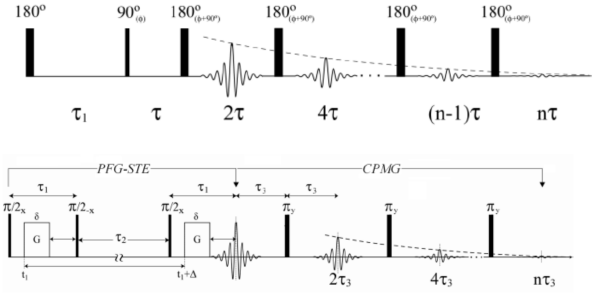

Figure 1: Pulses sequence for bidimensional T1-T2 and D-T2 experiments (Souza, 2012).

To convert the decay functions into T2 distribution we used the Inverse LaPlace transform (ILT) implemented in an in-house program developed by the São Carlos Nuclear Magnetic Resonance Laboratory, University of São Paulo/Brazil. For constructing the bidimensional maps, we utilized a patented MATLAB routine developed by Schlumberger. NMR measurements were performed in a RedstoneTM Tecmag spectrometer with 2MHz 1H (0.047T) magnet and a RedstoneTM Tecmag spectrometer with 85MHz 1H (2T) Oxford Instruments magnet for T2 distributions, both from the São Carlos Nuclear Magnetic Resonance Laboratory (USP).

Results and discussion

Transmitted-light optics

In this study we analyzed 11 thin sections of 8.60 m of core taken from Água Grande Formation sandstones. Three petrofacies have been defined (Figure 2) and also the porosity (Leite et al., 2014): 1) eolian (7536 sample); 2) fluvio-eolian (7545); 3) non reservoir (7562 sample).

Eolian petrofacies is composed of bimodal, well-sorted, parallel stratified fine to coarse subarkoses (Folk, 1968) which original average detrital composition is $Q_{93}F_6L_0$. Detrital quartz grains are monocrystalline grains. Feldspar grains are microcline, perthite and plagioclase. Accessory minerals include biotite, muscovite, epidote, cianite and zircon, while diagenetic constituents as caulinite, anatase and pirite appear filling the intergranular pore space. Primary minerals can be replaced by radiating fibrous intragranular chalcedony (< 0.5%). Other authigenic silica

present is quartz overgrowths cements which are developed on detrital quartz grains (av. 033%). These samples present low compactation rates and thus, have good porosity (av. 19.95%), and good permeability (av.49,3mD). It density is 2.63g/cm^3.

Fluvio-eolian petrofacies consists in moderate well-sorted medium to coarse sandstones interbedded with gradual parallel fine to very fine-grained subarkose. The detrital quartz and feldspar grains are similar to those of eolian petrofacies, except for the slightly higher plagioclase contents (av.4.1%). Diagenetic minerals are dickite, anatase, dolomite, albite and chalcedony. The presence of dicktite and anatase are the main cause of porosity-loss in these petrofacies. The porosity is in average 18,3% and permeability varies from low (4.14mD) to good (28,5mD) (av. 14,28mD) values.

Non-reservoir petrofacies consists of low porosity and low permeability subarkoses with low angle cross or parallel stratification. The primary minerals are quartz with undulose extinction, plagioclase and perthite while diagenetic minerals include dickite (~6,7%), illite/smectite, chlorite, anatase and pirite. Illite can replace the matrix or plagioclase. Clorite replaces biotite. The mud sandstone contains 75% of sand and 25% of mud.

Eolian and fluvio-eolian samples present anomalous porosity that is preserved due to the presence of microcrystalline quartz coats, while non-reservoir sample do not present it. (Leite et al., 2014).

Porosity (ϕ) and permeability (k)

Eolian (7536) and fluvio-eolian (7545) samples are classified as subarkoses. They present similar porosities (20.8 and 17.30 %, respectively), but their permeability is significantly different (34.30 and 4.14mD, respectively). The amount of clay minerals and diagenetic silica is higher in 7536 (5% illite/smectite, 0.33% chlorite and 0.66 diagenetic quartz) than in 7545 (3.3 % dickite and 0.33% diagenetic quartz). 7562 is the non-reservoir sample. It has low porosity and permeability and shows no microquartz coatings in quartz detrital grains and its diagenetic clay minerals content is the highest, comprising 6.67% dickite, 5% illite/smectite and 0.33% diagenetic silica.

According French & Worden (2013), anomalous porosity samples related to quartz coatings are characterized by the deposition of a chalcedony/amorphous nanofilm on top of detrital grains or on pre-existing overgrowth. The microcrystalline quartz deposited on top of this nanofilm inherits the c-axis orientation of the host grain, growing faster along this direction and thus preserving the pore space.

Magnetic susceptibility measurements

The magnetic susceptibility values are related with the clay content. Eolian and fluvio eolian samples have similar clay contents thus have similar magnetic susceptibility values, while the non revervoir sample is much more cemented, with the highest clay minerals contents and high magnetic susceptibility.

Nuclear Magnetic Resonance (NMR)

Pore size distributions

Figures 3a, 3b and 3c show T2 distribution map of 7536, 7545 and 7562 samples, respectively. Assuming a fast diffusion regime for the system, we can relate higher T2 values (slower magnetization decays) with larger pore sizes (Eq. 1 and Eq.2). Eolian and fluvio eolian samples have longer T2, while the non-reservoir sample has shorter T2. These data are consistent with petrographic results, since eolian samples present higher porosity and permeability and lower cementation, so we can interpret that the pore space was more preserved during the diagenesis processes.

T2 curves at 2 MHz show 4 modes. The small peak above 1 s corresponds to bulk water and probably results from excess of water at the surface of the samples during saturation process. In the literature, T2 values above 33 ms in sandstones are related to mobile water pore fillings, and are related to large pores, whereas values below 33 ms are related to the micropores which are filled by capillary bound water or clay bound water (Kenyon, 1997, Coates, 1999; but see also Dastidar et al., 2006). Here, the mode between 0.1 s and 1 s (T2 2 MHz curve) is related to water that fills the large pores (Figure 3a and 3b). Modes below 0.1 show some variability in microporosity in the 7536 sample (eolian), but show a bimodal behavior for small pores in 7545 sample (fluvio-eolian). The 7536 variability may result from the presence of clay-bound water (<0.01s T2) or from the presence of microporosity within the space among microcrystalline quartz grains (0.01-0.03 s T2) or both.

T2 curves at 85 MHz show some displacement of peaks to shorter times, likely due to the magnetic susceptibility influence on relaxation times. It results from the presence of pirite, biotite, epidote, anatase and Fe-bearing clay minerals. Although EDS analysis do not show clay minerals with Fe contents, chlorite coatings on the quartz grains have been described previously by Leite et al. (2014). The 7562 (non-reservoir) T2 Distribution curve shows predominant short times at 2 MHz and, consequently, a predominance of micropores and strong cementation.

In order to provide a comparative example, we also studied the NMR signal of Fontainebleau sandstones, which are homogenous rocks with well-characterized anomalous porosity (French & Worden, 2013). These rocks have very low magnetic susceptibility being thus less susceptible to field gradient effects. Accordingly, the displacement to shorter T2 times in Fontainebleau sandstones only occurs for the highest T2 values and in short times the 2 MHz and 85 MHz curves tend to be the same (Figure 3d).

Very high T2 times are dominant in Fontainebleau sandstones, but a microporosity can also be identified at shorter t values (Figure 3D). We can relate these two modes to large pores (high T2) and to the microporosity (low T2) of microcrystalline coats on host quartz grains as described by French & Worden (2013).

T1-T2 maps (Figure 4) indicate that 7562 sample has predominantly higher intensity on short T1 and T2 times, related to its smaller pores. Reservoir samples, on the other hand, present several partial distributions of T2 for

the same T1, for both short and long T2 (i.e small and large pores, respectively). This behavior was obtained also with 85MHz T1/T2 map for long T2 (not shown here) indicating possible high gradients caused by high magnetic susceptibility between fluid-grain or contents of paramagnetic minerals.

D-T2 maps (Figure 5) show that 7536, 7545 and the Fontainebleau sandstones have long T2 times which are close to the bulk water diffusion constant, compatible with the dominance of large pores in these rocks. The short T2 with low diffusion constant of all these samples, including the Fontainebleau, indicates restrict diffusion in the small pores. In Fontainebleau sandstones, which are almost completely devoid of clay this is caused by microporosity along the microcrystalline layer. By inference we suggest that the same mechanism also applies for the Recôncavo Basin samples. (Figures 3a,3b and 5a).

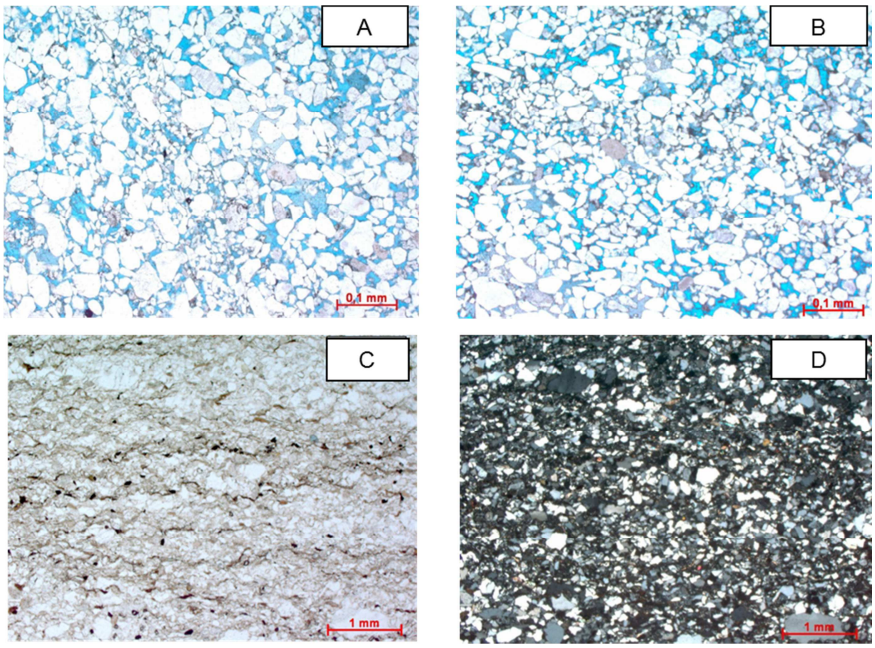

Figure 2: Geological texture using optical analyses of studied samples: a) eolian 7536; b) fluvio-eolian 7545; c) and d) non reservoir 7562.

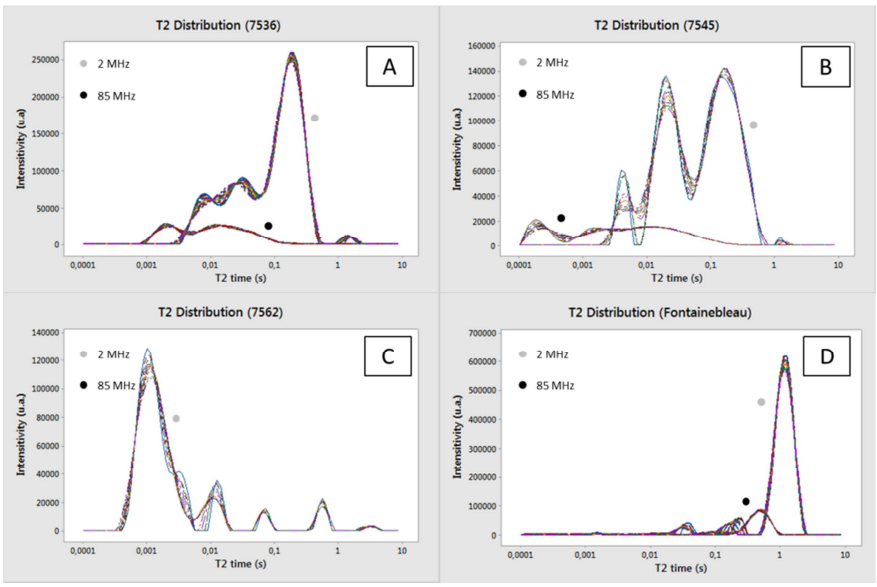

Figure 3: comparison among T2 distribution times.

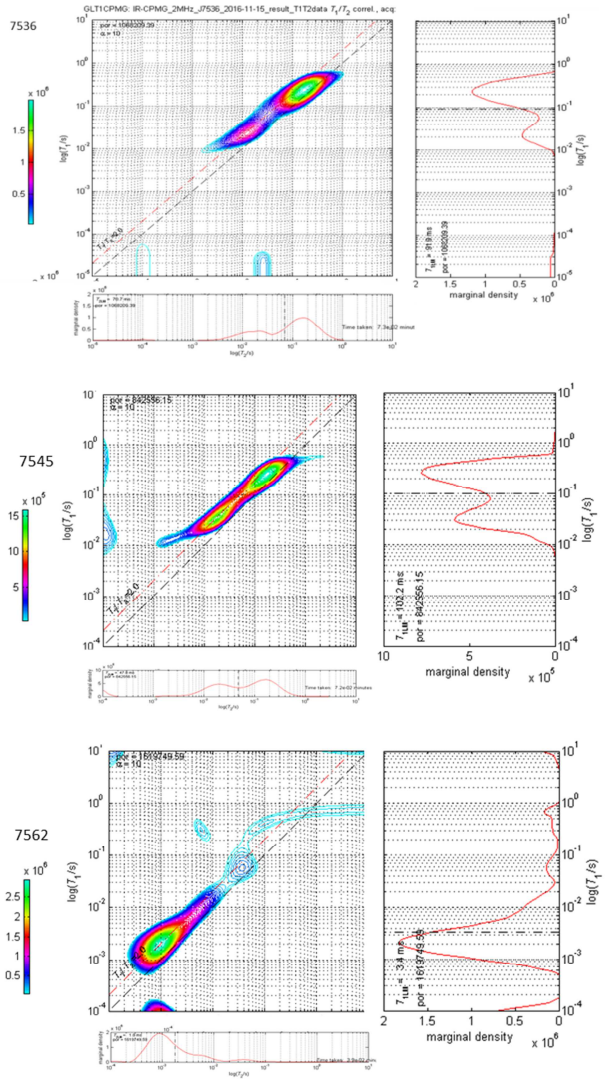

Figure 4: T1-T2 maps showing 7536 and 7545 the sigmoidal behavior of samples and, consequently, the spread T2 values for same T1 in small and large pores. Non reservoir samples 7562 show higher intensity of magnetization in small pores.

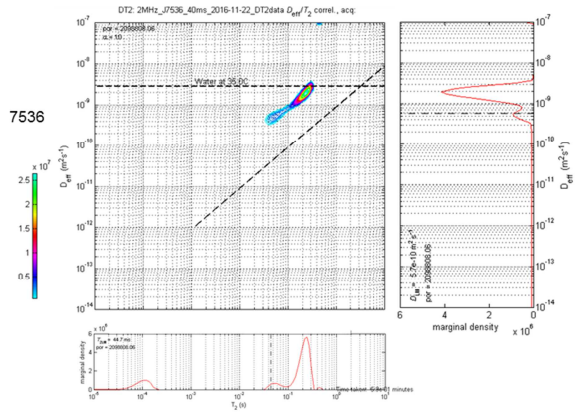

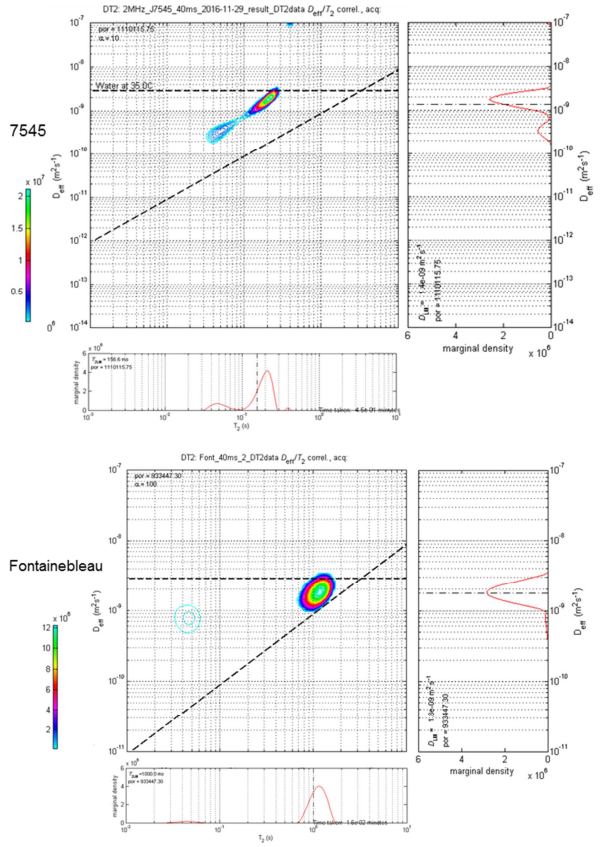

Figure 5: D-T2 maps showing the restrict diffusion for large pores (high T2 times at x axes) and small pores (short T2 times at x axes).

Conclusions

NMR T2 distributions suggest predominant large pores for Recôncavo reservoir sandstones and Fontainebleau sandstone, whereas the 7562 Recôncavo non-reservoir sandstone shows only short T2 times. The microporosity in Fontainebleau sample is originated at microcrystalline layers as shown T1/T2 and D/T2 maps. The eolian and fluvio-eolian samples of Recôncavo Basin (7536 and 7545) also contain microcrystalline quartz grains on host grain surfaces, which are the most likely cause of the short T2 values observed in these samples. Alternatively paramagnetic chlorite coats on quartz grains can also contribute to the signal.

Acknowledgments

CNPq scholarships for Marta Jacomo and Everton Oliveira. PETROBRAS and ANP for providing the samples and Schlumberger for the La Place inversion routines. PhD. Elton Montrazzi for support on NMR equipament assistence.

References

ANP (2016). Site: http://www.anp.gov.br/wwwanp/images/publicacoes/boletins-anp/boletim_de_outubro-2016.pdf. Acessado em 23/12/2016.

Bloch S., Lander R.H., Bonnell. Anomalously high porosity and permeability in deeply buried sandstone reservoirs? Origin and predictability. AAPG Bulletin.v.86.n.2. pp 301-328.

Coates G., Xiao L., Prammer M. 1999. *NMR logging: principles and applications*. Houston: Halliburton Energy Services Publication.

Cortez M.M.M. Análise geoestatística da geometria externa dos reservatórios fluvial e eólico da Formação Água Grande, área-central da Bacia do Recôncavo. Diss.mestrado UNICAMP. 1996.118p.

Dastidar R., Rai C.S., Sondergeld C.H., Shahreyar R. 2006. NMR Response of two clastic reservoirs: Influence of Depositional Environment. Petrophysics. Vol.47.n.3.p.214-222.

Folk, R. L., 1968. Petrology of sedimentary rocks. Austin, Texas (HemphilPs Book Store)

French M.W., Worden R.H. Orientation of microcrystalline quartz in the Fontainebleau Formation, Paris Basin and why it preserves porosity. 2013. Sedimentary Geology.pp149-158.

Hattori, I., Umeda, M., Nakagawa, T., Yamamote, H., 1996. From chalcedonic chert to quartz chert: diagenesis of chert hosted in a Miocene volcanic-sedimentary succession, Central Japan. Journal of Sedimentary Research, Section A: Sedimentary Petrology and Processes 66, 163–174.

Kenyon, W. 1997. Petrophysical principles of applications of NMR logging. Log Analyst, v.38, n.2,p43.

Leite C.M.M., Almeida J.R., De Ros L.F. Preservação de porosidade por microquartzo em reservatórios eólicos da Formação Água Grande na Bacia do Recôncavo, Bahia. 47.Congresso de Geologia.

Magnavita L.P., Szatmari P., Cupertino J.A., Destro N., Roberts D. The Recôncavo Basin. In: Regional Geology and Tectonics: Principles of Geologic Analysys. Editors: David G Roberts. A.W. Bally . Elsiever

Milani E. & Davison I. 1988. Basement control and transfer tectonics in theReconcavo-Tucano-Jatoba rift, Northeast Brazil. Tectonophysics, 154:41{50.

Mitchell J., Chandrasekera, T.C., Holland, D.J., Gladden L.F., Fordham, E.J. 2013. *Magnetic resonance imaging in laboratory petrophysical core analysis.* Physics Report 526. 165-225p.

Souza, A.A.D. *Estudo de propriedades petrofísicas de rochas sedimentares por Ressonância Magnética Nuclear*. 2012.Tese (Doutorado Ciência e Engenharia de Materiais)- Instituto de Física de São Carlos, Instituto de Química de São Carlos, Escola de Engenharia de São Carlos, Universidade de São Paulo, São Carlos, 236p.

Vincent, B., Fleury, M., Santerre, Y., Brigaud, B. 2011. *NMR relaxation of neritic carbonates: An integrated petrophysical and petrographical approach.* Journal of Applied Geophysics. 74(2011).38-58p.

Wiederkehr F. Análise tectono-estratigráficas das Formações Itaparica e Água Grande (Bacia do Recôncavo, Bahia). Diss de mestrado. UFGR. Porto Alegre. 2010. 100pp.

Worden R.H., French M.W., Mariani E. Amorphous silica nanofilms result in growth of misoriented microcrystalline quartz cement maintaining porosity in deeply buried sandstones. Geology.v. 40.n.2. 2012. pp.179-182.